

# Thermal Dileptons from Hot and Dense Strongly Interacting Matter

Hans J. Specht for the NA60 Collaboration

*Physikalisches Institut, Universität Heidelberg, Heidelberg, Germany*

**Abstract.** The NA60 experiment at the CERN SPS has studied muon-pair production in 158A GeV In-In collisions. The unprecedented precision of the data has allowed to isolate a strong excess of pairs above the known sources in the whole invariant mass region  $0.2 < M < 2.6$  GeV. The (mostly) Planck-like shape of the mass spectra, exponential  $m_T$  spectra, zero polarization and the general agreement with thermal-model results allow for a consistent interpretation of the excess dileptons as thermal radiation from a randomized system. For  $M < 1$  GeV, the process  $\pi^+ \pi^- \rightarrow \rho \rightarrow \mu^+ \mu^-$  dominates. The associated space-time averaged  $\rho$  spectral function shows a nearly diverging width in approaching chiral symmetry restoration, but essentially no shift in mass. Some in-medium effects are also seen for the  $\omega$ , but not for the  $\phi$ . For  $M > 1$  GeV, the average temperature associated with the mass spectrum is about 200 MeV, considerably above  $T_c = 170$  MeV, implying a transition to dominantly partonic emission sources in this region. The transition itself is mirrored by a large jump-like drop in the inverse slope of the transverse mass spectra around 1 GeV.

**Keywords:** Nuclear Collisions, Thermal Dileptons, Deconfinement, Hadrons in a Medium

**PACS:** 25.75.-q, 12.38.Mh, 13.85.Qk

## INTRODUCTION

At high temperature and baryon densities, QCD predicts strongly interacting matter to undergo a phase transition from hadronic constituents to a plasma of deconfined quarks and gluons. At the same time chiral symmetry, spontaneously broken in the hadronic world, is restored. High-energy nuclear collisions provide the only way to investigate this issue in the laboratory. Among the different observables used in this context, lepton pairs are particularly attractive. In contrast to hadrons, they directly probe the entire space-time evolution of the expanding fireball formed in such a collision, escaping freely without final-state interactions. At low invariant masses  $M < 1$  GeV (LMR), thermal dilepton production is largely mediated by the light vector mesons  $\rho$ ,  $\omega$  and  $\phi$ . Among these, the broad  $\rho$  (770) is by far the most important, due to its strong coupling to the  $\pi^+ \pi^-$  channel and its life time of only 1.3 fm, making it subject to regeneration in the much longer-lived fireball. It has therefore been considered since long as the prime probe for “in-medium modifications” of hadron properties, including even the QCD phase boundary itself [1-5]. At intermediate masses  $M > 1$  GeV (IMR), where hadronic spectral functions become increasingly uniform, Planck-like thermal radiation is expected from both hadronic and partonic sources. Dileptons with their independent variables mass and transverse momentum should be able to unambiguously differentiate between the two (unlike real photons).

Experimentally, excess dileptons above the known sources have been found and reported upon before [6-9], starting around 1995. A short review, including also the

preceding (very influential) pp era and theoretical milestones, has been published in [10]. Unfortunately, insufficient data quality in terms of statistics and mass resolution as well as the unclear role of non-thermal sources like open charm hindered final clarification on all fronts up to recently. A large step forward in technology, leading to completely new standards of the data quality in this field, has now been achieved by the “third-generation” experiment NA60 at the CERN SPS. The central results have already been published [11-17]. The present paper shortly reviews them, but places also particular emphasis on the quantitative understanding of the thermal-radiation part in connection with the medium modification of hadrons (one of the main topics of the workshop), just to create confidence towards a community which is usually exposed to “elementary” reactions rather than heavy-ion collisions.

## MAJOR ANALYSIS STEPS

The NA60 apparatus [15] combines the muon spectrometer previously used by NA10/NA38/NA50 with a novel radiation-hard, silicon-pixel vertex telescope, placed inside a 2.5 T dipole magnet between the target region and the hadron absorber. The matching of the muon tracks in the two spectrometers, both in coordinate and momentum space, greatly improves the dimuon mass resolution, reduces the combinatorial background from  $\pi$  and  $K$  decays, and allows to measure the dimuon offset with respect to the primary interaction vertex to tag open charm decays. The traditional high luminosity of dimuon in contrast to dielectron experiments is still conserved.

The data presented in this paper were taken for 158A GeV In-In collisions. The analysis was done in three major steps: assessment and subtraction of the background, identification of excess dimuons above the known sources and their subtraction from the latter, and full correction for experimental acceptance in all variables. The last two steps were never done in this field before and are thus unique to NA60.

The left panel of Fig.1 [11, 12] shows the opposite-sign, background and signal dimuon mass spectra, integrated over all collision centralities (determined by the track multiplicity in the Si telescope). The combinatorial background has been determined with an accuracy of about 1% by using a mixed-event technique [15], the much weaker background of incorrect (“fake”) matches between the two spectrometers by an overlay Monte Carlo method. After subtraction of the total background, the resulting net spectrum contains about 440 000 events, exceeding previous results by up to 3 orders of magnitude in effective statistics, depending on mass.

The enlarged LMR part of the net spectrum is shown in the middle panel of Fig.1 [11-14,16]. It is dominated by the known sources: the electromagnetic two-body decays of the completely resolved  $\eta$ ,  $\omega$  and  $\phi$  resonances, and the Dalitz decays of the  $\eta$ ,  $\eta'$  and  $\omega$ . While the peripheral “pp-like” data are quantitatively described by the sum of a “cocktail” of these contributions together with the  $\rho$  and open charm [12], this is not true for the more centrally weighted total data shown in Fig.1, due to the existence of a strong excess of pairs. The high data quality allows to isolate this excess with a priori *unknown characteristics* without any fits: the cocktail of the decay sources is subtracted from the total using *local* criteria which are solely based on the measured mass distribution itself. The  $\rho$  is not subtracted. The excess resulting from this difference formation is illustrated

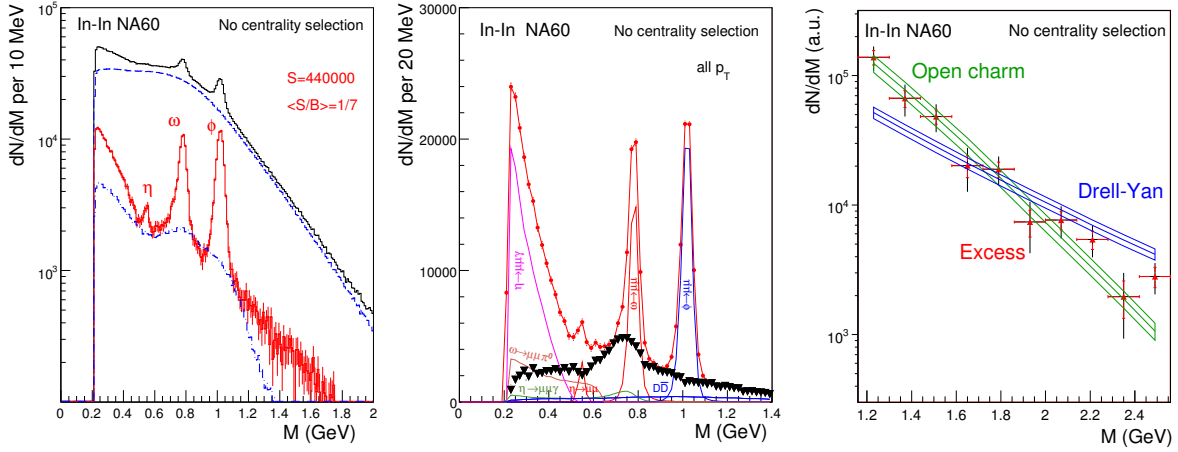


**FIGURE 1.** Left Panel: Mass spectra of the opposite-sign dimuons (upper histogram), combinatorial background (dashed), signal fake matches (dashed-dotted), and resulting signal (histogram with error bars). Middle Panel: Net mass spectrum before (dots) and after subtraction (triangles) of the known decay sources. Right panel: Centrality-integrated mass spectra of Drell-Yan, open charm and the excess dimuons (triangles), here already acceptance-corrected.

in the same figure. For  $p_T$  spectra, angular distributions and centrality dependences, the subtraction procedure is done in narrow slices of the respective variables (see [11-14] for details and error discussion). The subtracted data for the  $\eta$ ,  $\omega$  and  $\phi$  themselves are subject to the same further steps as the excess data.

The (extended) IMR part is shown in the right panel of Fig.1 [15]. The use of the silicon vertex tracker has allowed to disentangle prompt and offset dimuons resulting from simultaneous semi-muonic decays of (correlated)  $D$  and  $\bar{D}$  mesons. The results are perfectly consistent with no enhancement of open charm, but rather match the level expected from upscaling the NA50 results on charm in pA collisions. The excess observed in the IMR, confirming the result previously found by NA50, is really prompt, with an enhancement over Drell-Yan production of dimuons by a factor of  $2.4 \pm 0.08$  [15]. The excess can now be isolated in the same way as done in the LMR, by subtracting the expected known sources, here Drell-Yan and open charm as plotted in Fig.1, from the total data.

In the last step, the data are corrected for the acceptance of the NA60 apparatus and for the centrality-dependent pair reconstruction efficiencies. The acceptance shows strong variations with mass and  $p_T$  in the low-mass/low- $p_T$  region [12, 17], but is understood on the level of  $<10\%$ , based on a detailed study of the peripheral data [12] and a number of further investigations. In principle, the correction requires a 5-dimensional grid in  $M$ - $p_T$ - $y$ - $\cos\theta$ - $\cos\phi$  space ( $\theta$ ,  $\phi$  being the angles describing the dilepton angular distributions). This is neither realistic nor optimal. To avoid the large statistical errors connected with low-acceptance bins, the correction is usually done in 2-dimensional grids, using the measured distributions in the other variables as an input (examples  $M$ - $p_T$  [13, 16, 17] or  $y$ - $p_T$  [17] or  $\theta$ - $\phi$  [14]). This clearly requires an iteration procedure to become self-consistent, fortunately eased by an often only small sensitivity. It is of great importance,

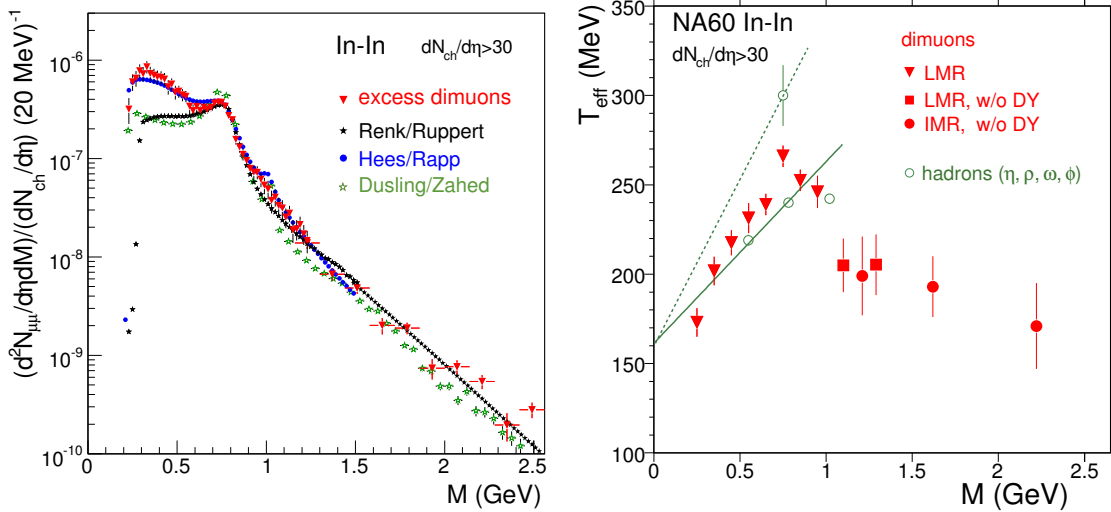


**FIGURE 2.** Left Panel: Acceptance-corrected invariant mass spectrum of the excess dimuons, integrated over  $p_T$ , compared with three different sets of thermal-model results in absolute terms. Right panel: Inverse slope parameter  $T_{\text{eff}}$  of the acceptance-corrected  $m_T$  spectra vs. dimuon mass (see [13] for a discussion of the statistical and systematic errors). Hadron results are shown for comparison.

however, to treat the different sources separately, i.e. *after* the subtraction procedure, due to differences in the distributions (open charm, e.g., is completely different).

## THERMAL RADIATION

The prime results on the excess data are summarized in Figs.2-4. The pure data aspects will be discussed first, followed by a coherent interpretation of all results in terms of thermal radiation further below. The left panel of Fig.2 shows the inclusive invariant mass spectrum of the excess dimuons for the complete range  $0.2 < M < 2.5$  GeV, with all known sources subtracted (except for the  $\rho$ ), integrated over  $p_T$ , corrected for experimental acceptance and normalized absolutely to the charged-particle rapidity density [18]. Compared to an earlier version of the figure [15], the errors have significantly decreased at low masses, using a 1-dimensional acceptance correction in  $M$  based on the measured correlated  $M$ - $p_T$  information ([16] and Fig.3). In addition, the subtraction of the narrow resonances is now based on an improved modeling of the experimental resolution [19], leading to a smoother spectral shape in the region of the  $\phi$ . The left panel of Fig.3 shows the associated  $m_T$  spectra for the LMR part, where  $m_T = (p_T^2 + M^2)^{1/2}$ . The normalization is arbitrary, allowing for an even spacing of the 10 spectra, but the absolute normalization of their integrals can directly be taken from the mass spectrum. In contrast to an earlier version of the figure [13, 15], the  $p_T$  coverage has mostly been extended to about 3 GeV. The  $m_T$  spectra for the IMR part are shown in the right panel of Fig.3 [15, 16]. All  $m_T$  spectra are, to a very high degree of accuracy [17], pure exponentials for  $(m_T - M) \geq 0.2$  GeV [13]. The complete information can therefore be condensed into one single parameter for each spectrum (determined with a very high accuracy), the

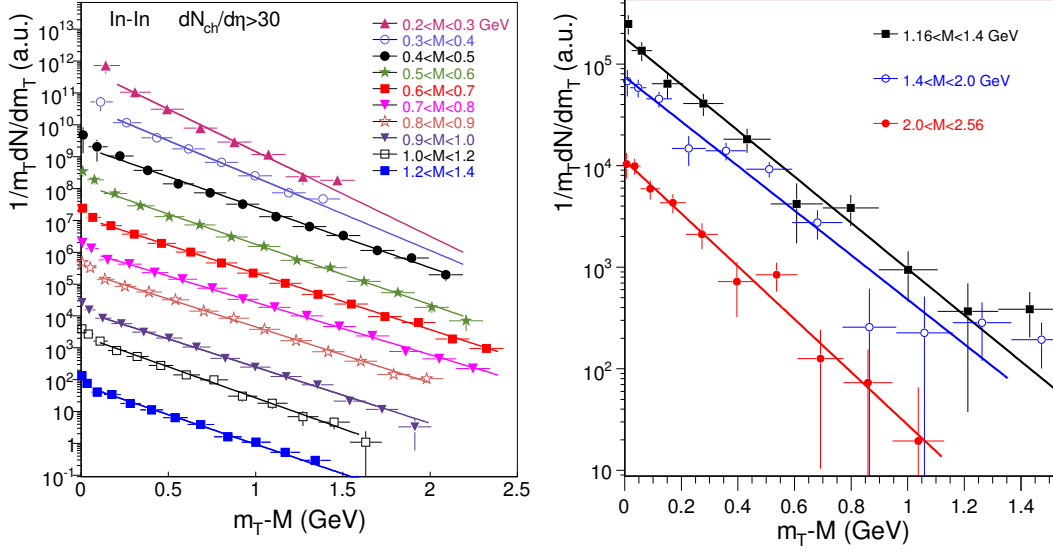


**FIGURE 3.** Left Panel: Acceptance-corrected  $m_T$  spectra of the excess dimuons for 10 mass windows in the LMR. Open charm is subtracted throughout. Right panel: Acceptance-corrected  $m_T$  spectra of the excess dimuons for 3 mass windows in the IMR.

inverse slope parameter  $T_{\text{eff}}$ , obtained by fitting the  $m_T$  data with the usual “ $m_T$ -scaling” expression  $1/m_T dN/dm_T \sim \exp(-m_T/T_{\text{eff}})$ . The resulting values of  $T_{\text{eff}}$  are plotted in the right panel of Fig.2 vs. dimuon mass. Above 1 GeV, the LMR data are corrected for DY to be consistent with the (independent) IMR analysis. To complement the information on  $M$  and  $p_T$ , Fig.4 finally shows the results from a systematic study of the dimuon angular distributions [14], another first in the field. Using the Collins-Soper reference frame (but the results are independent of that choice), all structure function parameters  $\lambda$ ,  $\mu$  and  $\nu$  (related to the spin-density matrix of the virtual photon) are found to be zero, and the projected distributions in  $|\cos\theta|$  and  $|\phi|$  are seen in Fig.4 to be uniform. This is a nontrivial result: the annihilation of quarks or pions along the beam direction, e.g., would lead to  $\lambda=+1$ ,  $\mu=\nu=0$  (lowest-order DY) or  $\lambda=-1$ ,  $\mu=\nu=0$ , corresponding to transverse and longitudinal polarization of the virtual photon, respectively.

Without resorting to any detailed theoretical modeling, the data themselves allow for a consistent global interpretation of the observed excess dimuons in terms of thermal radiation from the fireball. Three necessary prerequisites to justify the term are clearly fulfilled: (i) a Planck-like (nearly exponential) shape of the mass spectrum above 1 GeV, where the underlying spectral functions are expected to be uniform (as in the black-body case), (ii) purely exponential  $m_T$  spectra, and (iii) the absence of any polarization as expected for radiation from a randomized system.

Turning next to a more detailed discussion, the large drop of  $T_{\text{eff}}$  around masses of 1 GeV as seen in the right panel of Fig.2 is a strong hint for a qualitative change of the radiation from the LMR to the IMR. The mass region  $<1$  GeV has traditionally been associated with the process  $\pi^+\pi^- \rightarrow \rho \rightarrow \mu^+\mu^-$  as the dominant dilepton source. Indeed, the mass spectrum shows a considerable modulation, with clear signs for a

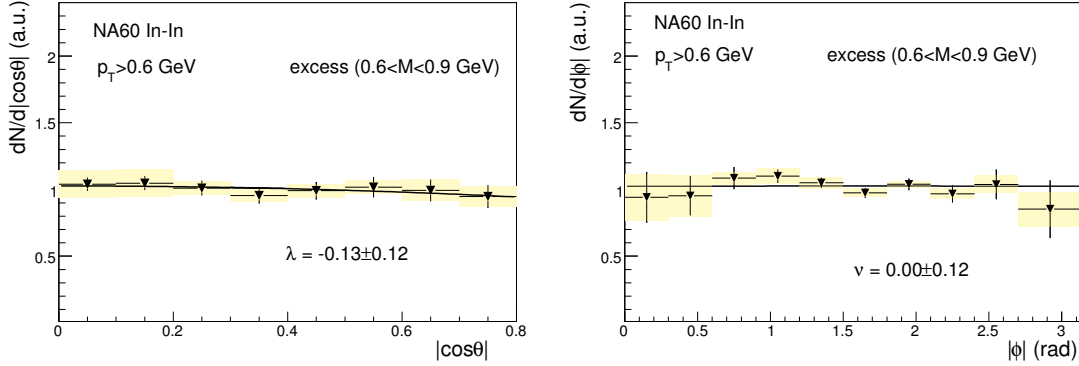


**FIGURE 4.** Acceptance-corrected polar (left) and azimuthal (right) angular distributions of the excess dimuons. The Collins-Soper reference frame has been used here. Analogous results have been obtained for the mass window  $0.4 < M < 0.6$  GeV [14].

(broadened)  $\rho$ . In the same region,  $T_{\text{eff}}$  shows a monotonic rise with mass all the way up to the nominal pole position of the  $\rho$ . This is a strong indication for radial flow of a “hadron-like” dilepton source, as confirmed by the genuine NA60 hadron data plotted in the same figure. The parameter  $T_{\text{eff}}$  can roughly be described by a superposition of a thermal and a flow part in the form  $T_{\text{eff}} \sim T + Mv^2$ , where  $v$  is the average flow velocity. Maximal flow is reached for the point with  $T_{\text{eff}} \sim 300$  MeV, obtained by isolating the peak part in the mass spectrum by a side-window subtraction method [16] and interpreted as the freeze-out  $\rho$  at the end of the fireball evolution, synonymous to the other hadrons. The maximal flow then mirrors the expected maximal coupling of the  $\rho$  to pions, while all other hadrons freeze out earlier, in quantitative support by a NA60 blast-wave analysis [20]. Extrapolating the trend of  $T_{\text{eff}}$  vs.  $M$  down to zero mass (and taking account of relativistic corrections for  $M < p_T$ ), the average temperature is found to be about 130-140 MeV in this region, considerably below  $T_c \sim 170$  MeV.

The interpretation of the mass region  $> 1$  GeV is quite straightforward, eased by an argument not placed before. Assuming flat spectral functions in the spirit of parton-hadron duality in the dilepton rates, the momentum-integrated yield is given by  $dN/dM \sim M^{3/2} \exp(-M/T)$ , where  $T$  reflects some space-time average over the system evolution. A fit of the mass spectrum with this expression over the range  $1.2 < M < 2.0$  GeV gives  $T = 205 \pm 12$  MeV. Since  $M$  is by construction a Lorentz-invariant, the mass spectrum is immune to any motion of the emitting sources, unlike  $m_T$  spectra or Planck’s law itself. The parameter  $T$  in the spectral shape of the mass spectrum is therefore purely thermal. The fit value of about 200 MeV, considerably above  $T_c \sim 170$  MeV, thus directly implies partonic emission sources to dominate in the IMR. This is fully consistent with an independent argument placed by NA60 from the beginning [13, 16]: the striking jump-like drop in  $T_{\text{eff}}$  around 1 GeV visible in Fig.2 can never be created by a continued hadronic scenario, but reflects early emission with a possible connection to the soft point in the equation-of-state as obtained from lattice QCD (most relevant at SPS energies). In the partonic scenario, flow can hardly develop up to  $T_c$ . This is reflected by the same average value of about 200 MeV seen in the  $T_{\text{eff}}$  plot beyond 1 GeV, with no margin left for

flow within the errors of 10-20 MeV, not to speak about any rising mass dependence in this region. These rather clear conclusions also end the years-long discussion on hadron-parton duality, where duality in the rates has been incorrectly taken over as duality in the yields, ignoring the differences in the space-time integration for partons and hadrons.

The three sets of thermal model results [21-23] which are also plotted in the left panel of Fig.2 largely confirm the above observations. To the extent that they roughly agree both with the shape and the absolute magnitude of the data, they present a fourth strong argument supporting the interpretation of the excess dimuons as thermal radiation. In particular, the agreement of the Hees/Rapp scenario [22] with the data in the region of the  $\rho$  spectral function is really spectacular, as shown even more clearly in a paper by Rapp presented at this Workshop [24]. In the region above 1 GeV, all three models explicitly differentiate between partonic and hadronic processes. In case of [21, 23], partons dominate, and the data are fully described up to 2.5 GeV. The average temperature associated with these two scenarios is 217 MeV (compared to the measured  $205 \pm 12$  MeV), with a small increase of the local values by about 10% towards higher masses. Partons also dominate in a further scenario not contained in Fig.2 [25]. In case of [22] however, hadrons dominate, with corresponding lower values of T, but the predictions stop at 1.5 GeV, too low to completely bear out the resulting conflict with the data in the region up to 2.5 GeV.

## VECTOR MESON SPECTRAL FUNCTIONS

The mediation of thermal radiation in the LMR by the vector mesons implies a convolution of the dilepton rate over the space-time evolution of the fireball, where the rate is given by the photon propagator, phase space factors and the vector meson spectral functions [5]. In case of the narrow  $\omega$  and  $\phi$ , the convolution hardly affects the line shape, and these mesons can therefore be isolated in a straightforward way. In case of the broad  $\rho$ , however, in particular if further broadened in the medium, the spectral shape is completely masked by the convolution procedure as seen in Fig.2, where the dilepton yield even increases further below the nominal pole of the  $\rho$ . Unfolding the final result is plainly impossible. A realistic way to at least project out the space-time averaged  $\rho$  spectral function is the use of a suitable correction function in 2-dimensional M- $p_T$  space. By a strange coincidence of suitable conditions, the experimental acceptance of NA60, being strongly reduced in the low-mass/low- $p_T$  region [12, 17], provides such a correction function in an unexpectedly perfect way. The left panel of Fig.5 proves the point [12]. Thermal radiation with an underlying uniform spectral function, using a full (uncut)  $p_T$  spectrum with an inverse slope parameter  $T_{\text{eff}}$  representative for the average, is transformed after propagation through the acceptance into again a uniform spectrum up to about 1 GeV, within 10%. In other words, the steep rise of the thermal spectrum due to the photon propagator and the Boltzmann factor is just about compensated by the falling acceptance in this region. Variations of the input  $p_T$  spectrum within reasonable physics limits affect the flatness of the output by at most 20%.

The right panel of Fig.5 shows the excess data in the LMR as directly measured, i.e. before correction for acceptance [11, 16]. This then can be interpreted as the in-medium  $\rho$  spectral function, averaged over space-time and momenta. In order to compare to

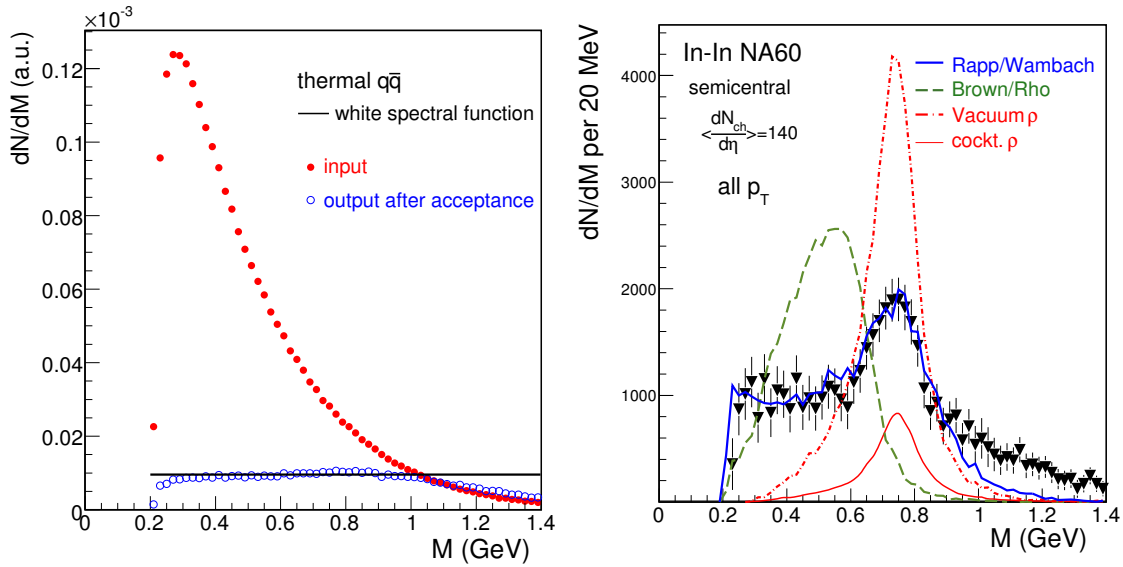


**FIGURE 5.** Left panel: Propagation of thermal radiation based on a uniform spectral function through the NA60 acceptance. The resulting spectrum is also uniform (see text). Right panel: Excess dimuons before acceptance correction, reflecting the in-medium  $\rho$  spectral function averaged over space-time and momenta. The theoretical predictions also shown are renormalized to the data for  $M < 0.9$  GeV. Beyond 0.9 GeV, other physical processes take over.

theory, a centrality selection of  $110 < dN_{ch}/d\eta < 170$  has been applied, but the data are very close to the inclusive data ( $\langle dN_{ch}/d\eta \rangle = 120$ ) with their much better statistics, contained in the middle panel of Fig.1. The evolution of the  $\rho$  spectral function with centrality is discussed in [12, 16]. A peaked structure is always seen, broadening strongly with centrality, but remaining essentially centered around the nominal pole position of the  $\rho$ . The *rms* of the distributions increases monotonically from that of a free  $\rho$  to almost the value of a uniform spectrum. The total yield relative to the (estimated) cocktail  $\rho$  increases by a factor of 6-7, reflecting the “ $\rho$ -clock” [26], i.e. the number of  $\rho$  generations created during the fireball evolution.

Fig.5 also contains the two main theoretical scenarios developed historically for the in-medium spectral properties of the  $\rho$ , dropping mass [2] and broadening [5], evaluated here for the same fireball evolution [27]. The model results are normalized to the data in the mass interval  $M < 0.9$  GeV, just to be independent of the fireball evolution. The unmodified  $\rho$  is clearly ruled out. The broadening scenario gets remarkably close, while the dropping mass scenario completely fails. This ends a decades-long controversy about the spectral properties of hadrons close to the QCD phase boundary, kept active solely through insufficient data quality. The connection to chiral symmetry restoration remains an open theoretical issue, but the way chiral partners ultimately mix is probably answered with “complete melting”.

In nuclear collisions, the longer-lived  $\omega$  (23 fm) and  $\phi$  (46 fm) have historically received much less attention than the  $\rho$ , since most of their dilepton decays occur after thermal freeze-out. The  $\omega$  suffers, on top, from the strong masking by the much more abundant (regenerated)  $\rho$ , leaving precision work rather to cold nuclear matter



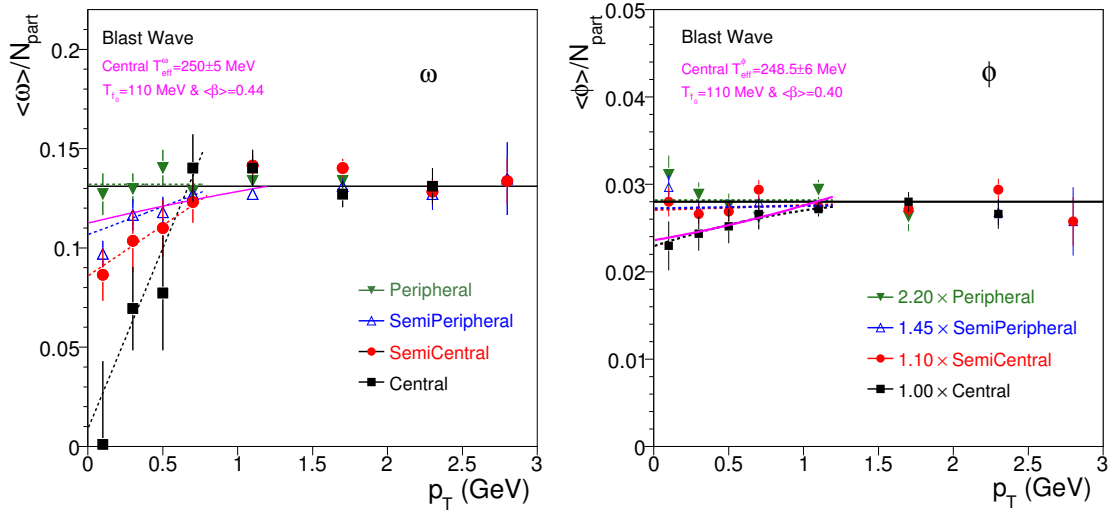


**FIGURE 6.**  $p_T$  dependence of the normalized yields of the  $\omega$  (left) and  $\phi$  (right) for 4 different centralities. The solid lines for  $p_T \leq 1$  GeV below the reference lines show the results from blast wave fits for central collisions. The dotted lines are only meant to guide the eye. The errors are purely statistical; the systematic errors are negligibly small compared to the statistical ones.

experiments. NA60 has addressed the  $\omega$  in a way directly coupled to the cocktail subtraction procedure. Due to the high mass resolution, the *disappearance* of the yield at low  $p_T$  out of the narrow  $\omega$  peak in the nominal pole position can sensitively be detected. The *appearance* of the yield elsewhere in the mass spectrum, originating from a mass shift or broadening or both is practically inaccessible, due to the masking by the  $\rho$ . Evidence for the disappearance of the  $\omega$  has been found by the following procedure [16]. The  $m_T$  spectrum, measured to be a pure exponential for  $(m_T - M) \geq 0.6$  GeV, is fit with the usual  $m_T$ -scaling expression used before, defining a reference line. The line is extrapolated to  $(m_T - M) = 0$ , and the ratio data/reference line is then used to monitor shape changes over the complete range in  $m_T$ . The procedure is done separately for four centrality bins. The results are shown in the left panel of Fig.6 [16], absolutely normalized to the full phase space ratio  $\omega/N_{part}$ . The effects of disappearance are quite striking: (i) a suppression of the relative yield below the reference line only occurs for  $p_T \leq 1$  GeV; (ii) there is a very strong centrality dependence of the suppression, reaching down to  $\leq 0.5$  of the reference line (the large errors reflect the increasing masking by the  $\rho$ ); (iii) the suppression effects are much larger than expected for the spectral distortions due to the blue shift from radial flow at low  $m_T$ ; a simulation on the basis of the blast wave analysis [20] shows at most 10% effects for central collisions. Thus, strong in-medium effects also exist for the  $\omega$ , but it seems impossible to clarify their nature within the NA60 frame.

The results from the same procedure applied to the  $\phi$  are shown in the right panel of Fig.6. No effects are seen beyond the limit set by the blast wave analysis. A precision analysis of the position and line shape of the  $\phi$ , the most isolated and therefore “easiest” hadron case in the NA60 data, has also been performed [19]. The mass and width are

found to be compatible with the PDG values at any centrality and at any  $p_T$ ; no evidence for in-medium modifications is observed.

## CONCLUSIONS

The precision of the NA60 data has set new standards in this field. This has allowed to consistently interpret the results in terms of thermal radiation, including identification of the two major sources. Theoretical modeling has matched this precision for the in-medium  $\rho$  spectral function, but not yet for a description of the dynamics. It is hoped that the strong constraints placed by these aspects of the data will contribute towards convergence, including the (theoretically) still controversial dominance of partons in the IMR already at SPS energies.

## REFERENCES

1. R. D. Pisarski, Phys. Lett. **110B**, (1982) 155; Phys. Rev. D **52**, R3773 (1995).
2. G. E. Brown, M. Rho, Phys. Rev. Lett. **66**, 2720 (1991); G. Q. Li, C. M. Ko and G. E. Brown, Phys. Rev. Lett. **75**, 4007 (1995); G. E. Brown and M. Rho, Phys. Rept. **363**, 85 (2002).
3. T. Hatsuda and S. H. Lee, Phys. Rev. C **46**, 34 (1992).
4. C. A. Dominguez, M. Loewe and J. C. Rojas, Z. Phys. **C59**, 63 (1993).
5. G. Chanfray, R. Rapp and J. Wambach, Phys. Rev. Lett. **76**, 368 (1996); R. Rapp, G. Chanfray and J. Wambach, Nucl. Phys. **A617**, 472 (1997); R. Rapp and J. Wambach, Adv. Nucl. Phys. **25**, 1 (2000).
6. G. Agakichiev *et al.* (CERES Collaboration), Eur. Phys. J. **C41**, 475 (2005) and earlier ref.
7. D. Adamova *et al.* (CERES Collaboration), Phys. Lett. B **666**, 425 (2008).
8. M. C. Abreu M C *et al.* (NA38/NA50 Collaboration), Nucl. Phys. A **698**, 539 (2002) and earlier ref.
9. A. L. S. Angelis *et al.* (HELIOS-3 Collaboration), Eur. Phys. J. C **13**, 433 (2000) and earlier ref.
10. H. J. Specht, Nucl. Phys. A **805**, 338 (2008), arXiv:0710.5433 [nucl-ex].
11. R. Arnaldi *et al.* [NA60 Collaboration], Phys. Rev. Lett. **96**, 162302 (2006).
12. S. Damjanovic *et al.* [NA60 Collaboration], Eur. Phys. J. C **49**, 235 (2007).
13. R. Arnaldi *et al.* [NA60 Collaboration], Phys. Rev. Lett. **100**, 022302 (2008).
14. R. Arnaldi *et al.* [NA60 Collaboration], Phys. Rev. Lett. **102**, 222301 (2009).
15. R. Arnaldi *et al.* [NA60 Collaboration], Eur. Phys. J. C **59**, 607 (2009).
16. R. Arnaldi *et al.* [NA60 Collaboration], Eur. Phys. J. C **61**, 711 (2009).
17. S. Damjanovic *et al.* [NA60 Collaboration], Nucl. Phys. A **783**, 327 (2007).
18. S. Damjanovic, R. Shahoyan and H. J. Specht, CERN Cour. **49N9** 31 (2009).
19. R. Arnaldi *et al.* [NA60 Collaboration], Eur. Phys. J. C **64**, 1 (2009).
20. R. Arnaldi *et al.* [NA60 Collaboration], J. Phys. G **37**, 094030 (2010).
21. T. Renk and J. Ruppert, Phys. Rev. C **77**, 024907 (2008); J. Ruppert *et al.*, Phys. Rev. Lett. **100**, 162301 (2008).
22. H. van Hees and R. Rapp, Nucl. Phys. A **806**, 339 (2008).
23. K. Dusling, D. Teaney and I. Zahed, Phys. Rev. C **75**, 024908 (2007); K. Dusling and I. Zahed, Phys. Rev. C **80**, 014902 (2009).
24. R. Rapp, arXiv:1010.1719 [nucl-th], these proceedings.
25. O. Linnyk, E. L. Bratkovskaya and W. Cassing, Nucl. Phys. A **830** 491C (2009).
26. U. W. Heinz and K. S. Lee, Nucl. Phys. A **544**, 503 (1992).
27. R. Rapp, (2003), private communication and R. Rapp, nucl-th/0204003.